# Effect of isotopic substitution on the visible absorption spectrum of ozone

Stuart M. Anderson, John Maeder, and Konrad Mauersberger

Citation: The Journal of Chemical Physics **94**, 6351 (1991); doi: 10.1063/1.460313
View online: http://dx.doi.org/10.1063/1.460313
View Table of Contents: http://scitation.aip.org/content/aip/journal/jcp/94/10?ver=pdfcov
Published by the AIP Publishing

# Effect of isotopic substitution on the visible absorption spectrum of ozone

Stuart M. Anderson
*Department of Physics, Augsburg College, Minneapolis, Minnesota 55454*

John Maeder and Konrad Mauersberger
*School of Physics and Astronomy, University of Minnesota, Minneapolis, Minnesota 55455*

(Received 30 November 1990; accepted 31 January 1991)

Absorption spectra for $^{16}O_3$ and $^{18}O_3$ have been recorded to study the vibronic structure of the Chappuis band. The isotope shifts indicate that the strongest features involve transitions to two electronically excited states characterized by adiabatic energies $\approx 750\ cm^{-1}$ apart, with the higher one near 16 400 $cm^{-1}$. The vibrational structure can be associated with a relatively simple progression in this higher state ($\omega_1$ and $\omega_2 \approx 1210$ and 640 $cm^{-1}$, respectively), and one isolated band associated with the lower state. Alternatively, an autocorrelation analysis indicates major recurrences near 31 and 41 fs for $^{16}O_3$, and correspondingly longer times for $^{18}O_3$. Minor recurrences at longer times are also present, but all are significantly shorter lived than those associated with the Hartley band. The results are discussed in the context of *ab initio* calculations and recent experimental and theoretical work involving visible and ultraviolet absorption spectra of ozone.

## I. INTRODUCTION

The fact that ozone absorbs weakly in the visible region was first noted by Chappuis over a century ago.[1] The spectrum has been recorded several times since then,[2-5] and appears as an irregular series of diffuse bands overlying a continuum. Its weak temperature dependence[5,6] has made it useful for monitoring atmospheric ozone from the ground[7] as well as from balloon platforms.[8] It has also been exploited in laboratory studies of photochemistry and molecular dynamics,[9] although relatively little is known about the identity of the electronic state (or states) involved.

Consideration of ozone's other absorption bands,[10] together with the results of *ab initio* calculations,[11,12] suggest that the Chappuis system is associated with an electronic transition to the $^1B_1$ state. This assumption has recently been questioned by Vaida *et al.*,[13] who observed significant differences between spectra of gas- and condensed-phase ozone. These were attributed to the participation of more than one electronically excited state in the transition. In this work we have recorded gas-phase spectra for $^{16}O_3$ and $^{18}O_3$ to provide new information on the electronic states responsible for the Chappuis bands. The technique is similar to that used by Katayama[14] to locate the origin of the Huggins band system, and more recently by us[15] to measure the adiabatic energy of the electronic state associated with the Wulf bands.

## II. APPARATUS AND PROCEDURE

The spectrometer has been described elsewhere.[15] Briefly, it is a computer-controlled, dual beam absorption instrument, providing a fractional absorption detection limit of $5 \times 10^{-4}$ with a path length of 46 cm. Neat ozone, produced either from high-purity natural abundance oxygen or 98 atom% $^{18}O_2$, was admitted to the sample cell at pressures of $\approx 40$ Torr at 298 K to provide peak optical depths of $\approx 0.3$. For this work the resolution determined from Ar and Hg lamp wavelength calibration spectra[16] was 2.3 nm FWHM. Absolute wavelength accuracy was $\pm 0.5$ nm, as indicated by spectra recorded for the atmospheric bands of $O_2$ near 762 nm.[17]

Spectra for $^{16}O$- and $^{18}O$-labeled ozone were recorded sequentially with a common calibration to minimize systematic wavelength errors in the isotope shifts. For convenience in analysis, their intensities were normalized to match at the peak of the strongest band near 602 nm (16 600 $cm^{-1}$). A typical pair is shown in Fig. 1(a). The signal to noise ratio decreased towards higher frequencies as both the lamp intensity and absorption cross sections decrease precipitiously. Consequently, data much beyond 21 000 $cm^{-1}$ become progressively more unreliable and were not used for studying the isotope effects.

## III. RESULTS

The shape of the $^{16}O_3$ spectrum we observe is in excellent agreement with that of Griggs.[4] Comparison of our spectra for $^{16}O_3$ and $^{18}O_3$ immediately suggests that the banded structure is due to vibrational progressions originating just to the red of the strongest band. The next most intense feature near 17 400 $cm^{-1}$, however, appears to shift slightly too much to fit this simple picture. The response of the spectrum to the red of 16 000 $cm^{-1}$ to isotopic labeling is also intriguing.

A more detailed examination was carried out by applying a running-mean subtraction filter to the spectra to enhance the vibrational structure. The process discriminates against features significantly broader or narrower than the apparent bands. We refer to it, therefore, as a "bandpass" filter (BPF). The effect is illustrated in the inset in Fig. 1(b), where we have applied it to a Lorentzian whose halfwidth



 0021-9606/91/106351-07$03.00  

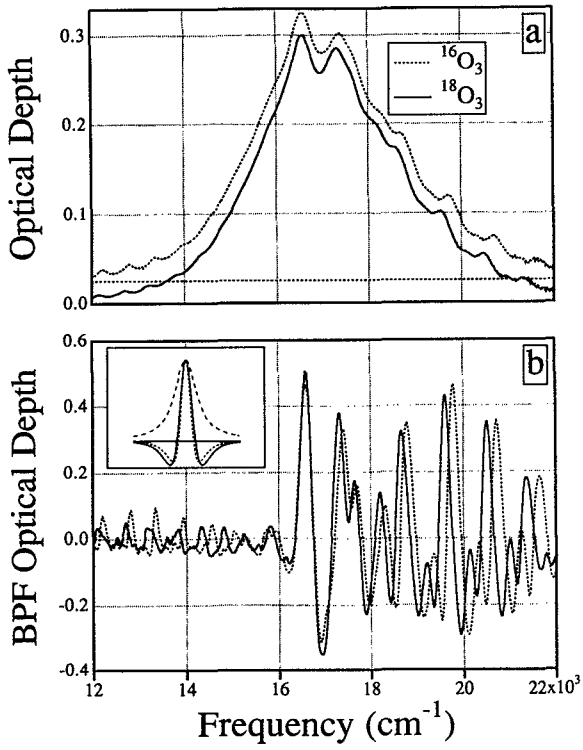


FIG. 1. (a) Measured absorption spectra for 40 Torr of $^{18}O_3$ (solid) and $^{16}O_3$ (dashed, displaced upward by 0.025 for clarity). Monochromator bandwidth (FWHM) was 63 cm$^{-1}$ at 16 600 cm$^{-1}$. (b) BPF versions of spectra shown in (a). Inset: illustration of digital filter used to enhance band structure; long dash = Lorentzian, short dash = 2nd derivative, solid line = Lorentzian after BPF processing.

resembles that of the bands in the ozone spectra. For comparison, the second derivative of the Lorentzian is also shown; the BPF is seen to be equivalent to a mildly broadened second derivative.

The results of filtering the ozone absorption spectra are shown in Fig. 1(b). The band structure is clear, and the anomalously large shift of the second peak is evident. Even the weaker bands become relatively well defined after filtering. One can also discern that some of the structure in the red wing arises from weak bands which suffer very large isotope shifts, and are very likely associated with the Wulf system studied previously.[15] We are currently investigating this region of the spectrum more closely. The band positions and related quantities determined from the BPF spectra for the larger features are listed in Table I, and discussed in the next section.

When full isotopic substitution is possible, interpretation of the resulting spectral shifts is straightforward since the frequencies of all vibrational modes in both electronic states decrease by a known factor.[14,18] The isotope shifts for the lowest members of a vibronic transition are approximately related to the total vibrational energies in the two electronic states:

$$\Delta\nu = \nu_{18} - \nu_{16} \approx (\rho - 1)(E'_v - E''_v), \qquad (1)$$

where $''$ denotes the lower state and $\rho = (m/m^*)^{1/2} = 0.942\,809$ for substitution of $^{16}O$ by $^{18}O$.[15] Since $\omega'_3$ should be small for a dissociative transition, $E'_0 < E''_0$ so that the lowest energy cold band would blueshift while higher energy bands should shift progressively to the red. A plot of isotope shift vs transition energy should yield a straight line of slope $\rho - 1$, which passes through zero when the vibrational energies in the two electronic states are equal. At this intercept the transition energy is equal to $\Delta E_a$, the adiabatic energy difference between the electronic states involved.

The isotope shifts determined from our spectra are presented in this fashion in Fig. 2. Two principal features are evident. First, there is a relatively clean progression associated with $\Delta E_a = 16\,500 \pm 150\,\text{cm}^{-1}$. These features are identified as 1–5*a* and 2–5*b* in Table I and are discussed further below. Second, there is the anomalously large shift associated with the intense band at 17 414 cm$^{-1}$; we denote this band by the symbol "*X*" in the table. A line of slope $\rho - 1$ drawn through this point suggests an adiabatic electronic energy 750 cm$^{-1}$ lower than that associated with the *a* and *b* bands.

TABLE I. Band positions, spacings and isotope shifts determined from bandpass filtered absorption spectra of Fig. 1(b). Spacings given for *a*–*a*, *b*–*b*, and *b*–*a* separations; i.e., 3*a*–2*a*, 3*b*–2*b*, and 2*b*–2*a* are 1076, 1041, and 606 cm$^{-1}$. Units are wave numbers in air, uncertainties are $2\sigma$, associated with locating the band centers. Absolute uncertainty in band locations is $\pm 10$ cm$^{-1}$.

| Band | $\nu_{16}$ | $\Delta\nu_{16}$ | $\nu_{18}$ | $\Delta\nu_{18}$ | $\nu_{18} - \nu_{16}$ |
|---|---|---|---|---|---|
| 1*a* | 16 600 ± 2 | 1114 ± 3 | 16 594 ± 2 | 1060 ± 3 | − 6 ± 3 |
| *X* | 17 414 ± 2 | ··· | 17 319 ± 2 | ··· | − 95 ± 3 |
| 2*a* | 17 714 ± 2 | 1076 ± 3 | 17 654 ± 2 | 1010 ± 3 | − 60 ± 3 |
| 2*b* | 18 320 ± 5 | 1041 ± 6 | 18 205 ± 2 | 998 ± 3 | − 115 ± 6 |
| | | 606 ± 6 | | 551 ± 3 | |
| 3*a* | 18 790 ± 2 | 1002 ± 3 | 18 664 ± 2 | 943 ± 3 | − 126 ± 3 |
| 3*b* | 19 361 ± 2 | 983 ± 3 | 19 203 ± 2 | 930 ± 3 | − 158 ± 3 |
| | | 571 ± 3 | | 539 ± 3 | |
| 4*a* | 19 792 ± 2 | 941 ± 3 | 19 607 ± 2 | 904 ± 3 | − 185 ± 3 |
| 4*b* | 20 344 ± 2 | 916 ± 3 | 20 133 ± 2 | 873 ± 3 | − 211 ± 3 |
| | | 552 ± 3 | | 526 ± 3 | |
| 5*a* | 20 733 ± 2 | ··· | 20 511 ± 2 | ··· | − 222 ± 3 |
| 5*b* | 21 260 ± 2 | ··· | 21 006 ± 2 | ··· | − 254 ± 3 |
| | | 527 ± 3 | | 495 ± 3 | |

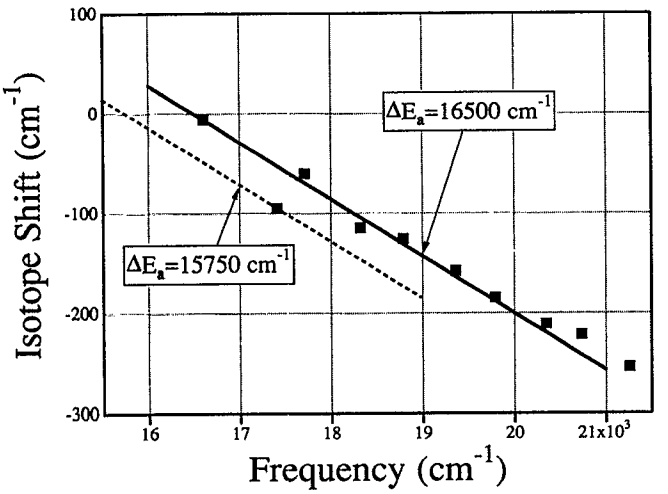


FIG. 2. Band peak isotope shifts ($\nu_{18} - \nu_{16}$) determined from peaks in Fig. 1(b) vs $^{16}O_3$ transition frequency. Lines have slope $\rho - 1$, correspond to pure electronic transition energies of 15 750 and 16 500 cm$^{-1}$.

## IV. DISCUSSION

### A. Electronic assignment

Although the isotope shifts we observe suggest that the two strongest vibronic features associated with the Chappuis system arise from transitions to different electronic states, we are not the first to propose this possibility. Vaida *et al.*[13] reported a similar conclusion based on marked differences between the visible absorption spectra of gas- and condensed-phase ozone. These included a large ($\approx$200 cm$^{-1}$) decrease in the spacing between bands 1*a* and *X*, and the appearance of two new features at 15 850 and 15 310 cm$^{-1}$ upon condensation.[19] The first effect was attributed to gas-solvent shifts, which are apparently controlled by the nature of the electronic states responsible for the transitions.[20] Remarkably, the two new bands appear near frequencies appropriate for transitions to an electronic state with the lower of the two adiabatic energies determined in the present work. Our observations are therefore consistent with those of Vaida *et al.*, and serve to strengthen the case for assigning the visible absorption bands of ozone to more than one electronic state.

To determine the likely identity of these states it is useful to compare the present results to the predictions of *ab initio* calculations. We have tabulated these previously,[15] and present them in Table II for convenience. In constructing this summary we have used Thunemann *et al.*'s values for vertical excitation energies[21] together with Hay and Dunning's calculations[12] of potential energy surfaces to obtain improved estimates of adiabatic energies. Note that Thunemann *et al.*'s results are in better agreement with experiment, and consistently lower (by a factor of 0.76 on the average) than Hay and Dunning's values. Estimated adiabatic energies (sixth column) were obtained by scaling Hay and Dunning's vertical–adiabatic energy differences to correct for this systematic offset and subtracting these from Thunemann *et al.*'s vertical energies. Our experimental adiabatic energies, 15 750 cm$^{-1}$ (1.95 eV) and 16 500 cm$^{-1}$ (2.05 eV) should be compared with this column of the table.

Our results are fairly close to the estimated energies for the 2 $^3B_2$, $^1B_1$, and $^3B_1$ states. Transitions from the $^1A_1$ ground state to each of these are dipole allowed, although those associated with the triplet states are spin forbidden and would therefore be quite weak barring significant mixing. The $^1A_1$ and $^1B_1$ states are predicted to have similar bond angles (117.7 vs 116°), but rather different bond lengths (1.30 vs 1.37 Å),[12] so that one would expect a simple, moderately long progression in $\nu_1$. This is consistent with what we observe here for the higher energy electronic state. It therefore seems that bands 1–5 (both *a* and *b*) could be associated with the $^1B_1$ state, and that band *X* may arise from mixing of the $^1B_1$ state with one of the two triplets. We are inclined to choose the 2 $^3B_2$, although the uncertainties in the estimated adiabatic energies together with the fact that we only observe a single isolated band precludes a definitive assignment.

Although this conclusion is conceptually similar to that reached by Vaida *et al.*,[13] it differs in the identity of the electronic states. They have suggested that the allowed transition is to the $^1A_2$ and that the lowest-lying triplets are responsible for the spectral anomalies. We have previously

TABLE II. Summary of electronic states of ozone. Vertical energies from Ref. 21; adiabatic energies estimated from scaled vertical–adiabatic differences given in Ref. 12 combined with vertical energies of Ref. 21 (see the text). Vertical experimental energies from Ref. 10, adiabatic from Refs. 14 and 15.

| State | Vertical energy | | Expt. | Adiabatic energy | | Expt. | Assignment |
|---|---|---|---|---|---|---|---|
| | Ref. 21 | Ref. 12 | | Ref. 12 | Estimated | | |
| $^1B_2$ | 1.20 | 1.60 | ··· | 0.92 | 0.68 | ··· | ··· |
| $^1A_2$ | 1.44 | 2.09 | ··· | 1.35 | 0.88 | ··· | ··· |
| $^1A_2$ | 1.72 | 2.34 | 1.6 | 1.66 | 1.20 | 1.24 ± 0.01 | Wulf bands |
| $^1B_1$ | 1.59 | 2.01 | ··· | 1.74 | 1.39 | ··· | ··· |
| $^1B_1$ | 1.95 | 2.41 | 2.1 | 2.06 | 1.68 | ··· | Chappuis bands |
| 2 $^1B_2$ | 3.27 | 4.71 | ··· | 2.92 | 1.91 | ··· | ··· |
| 2 $^1A_1$ | 3.60 | 4.58 | ··· | 1.20 | 1.04 | ··· | (ring state?) |
| $^1B_2$ | 4.97 | 6.12 | 4.9 | 5.54 | 4.53 | 3.41 | Hartley, Huggins Bands |

questioned this choice based on the existence of the Wulf bands,[15] but perhaps the best argument against it is the lack of any significant absorption feature between the Chappuis and Huggins bands. Such a feature would certainly be expected if the oscillator strength of the visible band is too small for a transition to the $^1B_1$ state and the Chappuis system were due to an even weaker $^1A_2 \leftarrow {}^1A_1$ transition. This does not mean that the $^1A_2$ makes *no* contribution in this region. Indeed, the large isotope shifts associated with the weak undulations to the red of the principal maximum imply that the transition responsible for the Wulf bands (which we take to be $^1A_2 \leftarrow {}^1A_1$) does affect the visible absorption spectrum to some extent.

This assignment does present some problems. First among them is the fact that the $^1B_1$ state correlates with $O(^1D) + O_2(^1\Delta)$, so that dissociation to these products is endothermic by $\sim 2$ eV throughout the visible region.[12] One should observe a highly structured bound–bound spectrum, but this does not appear to be the case.[6] Second, the nascent products of the photodissociation appear to be in their ground electronic states, namely $O(^3P) + O_2(^3\Sigma)$.[9] One could speculate that the $^1B_1 \leftarrow {}^1A_1$ transition is responsible for the oscillator strength and invoke some rapid internal electronic conversion process to allow dissociation, but it seems clear that a quantitative description of the electronic structure of this system will require a formidable theoretical treatment.[22] Nonetheless, it is interesting to analyze the vibrational structure assuming that a simple electronic assignment can be made.

### B. Vibrational analysis

The structure evident in these spectra have been analyzed using two complementary approaches. First, one may associate the vibrational bands with motions involving bound, normal mode degrees of freedom orthogonal to the dissociation coordinate. This is the spirit of previous assignments and our purpose here is to examine these in light of the isotope shifts we observe. Second, one may analyze the structure in terms of trajectories on the dissociative surface which bring some fraction of the wave packet back to its initial location. Although formal assignment of these recurrences requires accurate knowledge of the potential energy surface, one can still determine the periods of the dominant recurrences and get a qualitative picture of the dissociation. Both methods are discussed below.

#### *1. Normal mode approach*

At least one previous attempt to interpret the vibrational structure of the Chappuis system[9] has been influenced by the apparent need to account for the $X$ band. In the context of the present treatment, we exclude this feature from the analysis because it appears to be associated with a different electronic state. The remaining structure can be described reasonably well using conventional methods,[18] modified slightly to account for the dissociative nature of the transition as discussed by Pack.[23]

The band separations listed in Table I clearly fall into two groups, near 1000 and 575 $cm^{-1}$, respectively; not far from what one might expect for $\nu_1$ and $\nu_2$ frequencies in the excited state. Our labeling of the bands reflects this and suggests that the absorption peaks arise from vibronic transitions originating in the $^1A_1(0,0,0)$ state and terminating near vibrational levels associated with bound degrees of freedom on the upper surface,[22] which we denote by $(v_1', v_2')$. Choosing the minimum of the lower surface as a reference, these energies can be written as

$$T'' = E_0'' = 1/2 \sum_i \omega_i'' + 1/4 \sum_i \sum_{k>i} x_{ik}'' \tag{2}$$

and

$$T' = T_e' + \Delta E_f + \sum_i (v_i' + 1/2)\omega_i' + \sum_i \sum_{k>i} (v_i' + 1/2)(v_k' + 1/2)x_{ik}', \tag{3}$$

respectively. In these expressions $\omega_i$ and $x_{ik}$ are the usual harmonic and anharmonic constants, $T_e'$ is the adiabatic electronic energy of the upper surface, and $\Delta E_f$ is the initial photofragment kinetic energy associated with the dissociation coordinate. The photon energies are given by the difference between these, for each of $^{16}O_3$ and $^{18}O_3$:

$$\nu_{16} = T_e' + \Delta E_f + \sum_i (v_i' + 1/2)\omega_i' + \sum_i \sum_{k>i} (v_i' + 1/2)(v_k' + 1/2)x_{ik}' - E_0'' \tag{4}$$

$$\nu_{18} = T_e' + f(\rho)\Delta E_f + \rho \sum_i (v_i' + 1/2)\omega_i' + \rho^2 \sum_i \sum_{k>i} (v_i' + 1/2)(v_k' + 1/2)x_{ik}' - E_0''^*, \tag{5}$$

where $\rho = (m/m^*)^{1/2} = (16/18)^{1/2} = 0.942\,809$, and $E_0''^*$ is Eq. (2) for the isotopically labeled molecule.

The only unconventional feature of this description is the parameter $\Delta E_f$, which plays a role similar to that of $\omega_3'$ for a bound–bound transition. It represents the fact that maxima in the bound–free transition probability (corresponding to local absorption peaks) occur at photon energies slightly above the top of the barrier for dissociative motion on the upper electronic surface.[22] Apparent band locations are therefore associated with small positive values of this parameter.

Of particular interest here is the response of $\Delta E_f$ to isotopic substitution. The example originally treated by Pack[23] was similar to the present case in that the binding energy of the lower state was close to the barrier height of the upper state. By scaling his Fig. 5 result to energies appropriate for Chappuis band transitions ($\sim 1$ eV well depth and barrier height) we estimate $\Delta E_f$ to be roughly 80 $cm^{-1}$. When these calculations are repeated with isotopic substitution in mind[24] one finds that although the value of $\Delta E_f$ does depend on the height and breadth of the barrier, 80 $cm^{-1}$ is not an unreasonable ballpark estimate, and that $\Delta E_f$ decreases with mass such that $f(\rho) = \rho$ accounts for the change reasonably well.

Our analysis was carried out in two steps. First, the band

positions were fitted to quadratics in $v_1' + 1/2$ to obtain candidate assignments and estimates of the vibrational constants. Together with the adiabatic electronic energy determined above, these indicated that the $1a$ band can only arise from the $(v_1' = 0, v_2' = 1)$ state (consistent with its small isotope shift), and that the $b$ bands could be assigned as either $(v_1', v_2' = 0)$ or $(v_1', v_2' = 2)$. Second, these results were used as initial guesses for nonlinear least square fits to all band positions for $^{16}O_3$ *and* $^{18}O_3$ employing Eqs. (4) and (5) simultaneously. Assignment of the $b$ bands to $(v_1', v_2' = 2)$ produced the best fit, reproducing the observed band positions with an rms deviation of 8 $cm^{-1}$. This is somewhat larger than the uncertainty in the measured relative band positions. The parameters derived from the fit were: $T_e' = 16\,385 \pm 20$, $\omega_1' = 1213 \pm 5$, $\omega_2' = 638 \pm 5$, $\Delta E_J = 135 \pm 15$, $x_{11}' = -30 \pm 1$, $x_{12}' = -21 \pm 2$, and $x_{22}' = -4 \pm 2$, all in $cm^{-1}$.

In contrast, the harmonic frequencies predicted by *ab initio* calculations for the $^1B_1$ state are $\omega_1' = 965$ and $\omega_2' = 489$ $cm^{-1}$, and the anharmonic constants for the ground state of ozone are $x_{11}'' = -4.9$, $x_{12}' = -9.1$, and $x_{22}' = -1.0$ $cm^{-1}$. The latter discrepancy is not really surprising, since it may reflect real differences between the two potential energy surfaces. The anharmonic constants are probably not accurate due to the relatively small number of bands analyzed here. The fact that the experimentally determined harmonic frequencies differ by more than 25% from their theoretical counterparts is more troubling, and may indicate either a qualitative problem with our assignment or an inadequacy in the *ab initio* calculations.

A comparison with previous assignments of the Chappuis band structure is presented in Fig. 3. Levene *et al.*'s assignment was purely harmonic ($\omega_1' = 930$, $\omega_2' = 460$ $cm^{-1}$, all $x_{ik}' = 0$) and was apparently guided by a desire to account for the $X$ band. It implies that the strongest feature near 16 600 $cm^{-1}$ is the band origin, implying an isotopic blueshift; we observe a small shift to the red. Wulf's formula

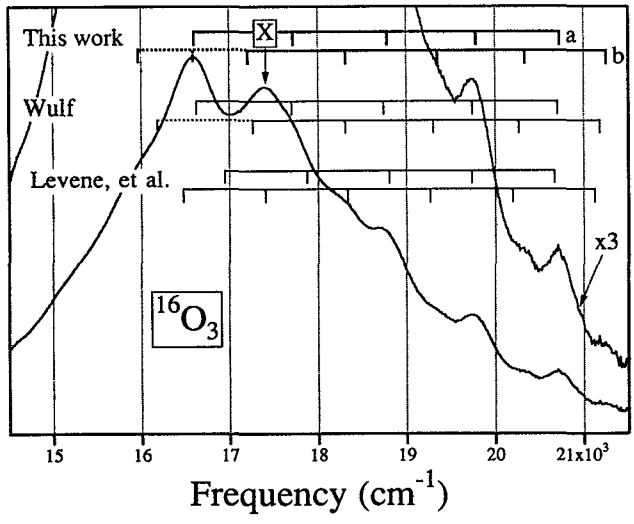


FIG. 3. Comparison of vibrational assignments derived in this work for $^{16}O_3$ with previous ones. The symbols "$a$", "$b$," and "$X$" refer to the designations in Table II. The band marked $X$ is excluded from our assignment.

for the band positions, $\nu = 16\,625 + n'(1099 - 20n') - 435n''$ (with $n'' = 0$ and 1), is in strikingly good agreement with our assignment, though it is not clear where he placed the band origin. The only substantive difference between Wulf's assignment and ours is that we associate the $b$ bands with transitions to $(v_1', v_2' = 2)$ rather than $(v_1', v_2' = 0)$. *It is remarkable that his assignment correctly leaves out the X band.* Our results suggest that the transition to the $(v_1' = 0, v_2' = 0)$ state is near 15 980 $cm^{-1}$, a region which may be complicated by the involvement of several electronic states.

### 2. Recurrence approach

The presence of vibrational structure in continuous spectra can also be understood in dynamic terms, as arising from temporal variations in the overlap between initial and time-evolving wave packets on the upper state surface.[25] Peaks in this overlap, or autocorrelation function, correspond to classical trajectories which return to that part of the surface where the dissociative motion began, though not necessarily to normal mode motions. Application of this approach to the Hartley bands, made possible in large measure by the availability of an accurate $^1B_2$ potential energy surface, has produced the first quantitative account of the small oscillations present in that spectrum.[26] Such a treatment obviously cannot be carried out in the present case. Nonetheless, it is useful to examine the spectrum in this fashion, particularly in comparison with the Hartley band results.

As described elsewhere,[25,26] the autocorrelation function is related to the absorption spectrum through a Fourier transformation:

$$\langle \Phi(0) | \Phi(t) \rangle \propto e^{-iE''t} \int e^{-i\omega t} \varepsilon(\omega)/\omega \, d\omega, \qquad (6)$$

in which $E''$ is the rovibrational energy of the ground state and $\varepsilon(\omega)$ is the absorption cross section. Evaluation of the integral was performed by first constructing spectra sampled at equally spaced frequency intervals from those of Fig. 1(a) by linear interpolation, and then applying standard FFT techniques. The results are presented in Fig. 4, which shows the absolute value of the autocorrelation function as a function of time for $^{16}O_3$ and $^{18}O_3$, normalized to unity at $t = 0$. The uncertainties are indicated by the size of the plotted points.

Following the initial drop, which occurs in about 10 fs, we observed peaks for $^{16}O_3$ at 31 and 41 fs that shift to later times under isotopic substitution. The magnitude of the shift (about 2 fs) is consistent with a simple $\sqrt{m/m^*}$ decrease in velocity. The first peak corresponds to a vibrational frequency of 1100 $cm^{-1}$, and probably derives from the $a$–$a$ band spacings. The second peak corresponds to a vibrational frequency of 800 $cm^{-1}$, and is most likely related to the spacing between the $1a$ and $X$ bands. Subsequent smaller peaks are evident in the vicinity of 60 fs, but the connection between the $^{16}O_3$ and $^{18}O_3$ features is less clear. These correspond to vibrational frequencies between 500–600 $cm^{-1}$, and could be related to the $b$–$a$ spacings and/or the remnants of the Wulf bands.

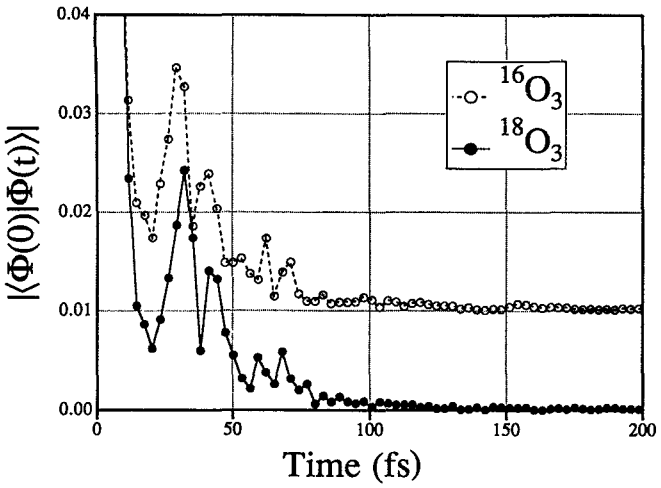


FIG. 4. Amplitude of the autocorrelation functions derived from the spectra of Fig. 1(a) normalized to unity at $t = 0$. Temporal resolution is transform limited. Solid symbols for $^{18}O_3$, open symbols for $^{16}O_3$. The latter has been displaced vertically for clarity.

Comparison of these results with those for the Hartley band[26] reveals some striking differences between the visible and ultraviolet dissociation events. First, the initial decay derived from the Hartley band (6 fs) is more rapid than what we observe here (10 fs), indicating that the $^1B_2$ surface is considerably steeper where the wave packet starts out than is the surface associated with the Chappuis system. This is reflected in the greater width of the Hartley continuum, and is consistent with the large difference between the vertical and adiabatic energies of the $^1B_2$ state. Second, the recurrences associated with uv absorption persist much longer than those shown in Fig. 4. In our case the autocorrelation function amplitude drops to $10^{-3}$ by 80 fs and falls relatively smoothly by another order of magnitude by 170 fs. By comparison, the recurrences associated with the Hartley band continue to 130 fs followed by a plateau which drops off abruptly at 240 fs. This suggests that the upper surface for the visible transitions is relatively simple, reducing the likelihood of complicated, long-period trajectories. Finally, the intensity of the recurrences found by Johnson and Kinsey[26] are five times weaker than those observed here. This corresponds to the fact that the Chappuis band structure is simpler and more pronounced, and means that more of the wave packet returns to its point of origin. One would, of course, expect this if the recurrence times are relatively short since the packet would not have had as much time to spread before returning.

A quantitative analysis would require a systematic search for quasistable trajectories whose periods match the recurrence times indicated in Fig. 4. The autocorrelation functions are presented here partly in the hope that the required information, namely an accurate potential energy surface, will soon become available. It would be particularly interesting to better understand the peaks near 60 fs, which do not appear to respond simply to isotopic substitution.

## V. CONCLUSION

Analysis of absorption spectra for $^{16}O_3$ and $^{18}O_3$ in the visible region provides new information on the electronic and vibrational structure of the Chappuis bands. Our results are consistent with those deduced from anomalies in the absorption spectrum of condensed-phase ozone, i.e., that the two strongest features may be associated with different electronically excited states. Within a conventional description of the vibrational structure the adiabatic energies of these two states are separated by about 750 $cm^{-1}$. The higher state lies near 16 400 $cm^{-1}$, and is responsible for most of the observed vibrational structure with $\omega_1$ and $\omega_2 \approx 1210$ and 640 $cm^{-1}$, respectively; the lower state produces the band at 17 414 $cm^{-1}$ and could be responsible for the condensed-phase observations. An examination of the spectra in terms of their corresponding autocorrelation functions has also been carried out. The dominant recurrences at 31 and 41 fs clearly show the expected $\sqrt{m/m^*}$ isotope shift while the weaker ones near 60 fs do not. Comparison with a similar study of the Hartley band provides some qualitative information about the characteristics of the upper state surface(s) responsible for the Chappuis system.

Our results suggest a number of directions for future work. First, measurement of the isotope shifts associated with the visible absorption bands of condensed-phase ozone would help to determine the adiabatic energy of the electronic state responsible for these anomalies. On the basis of the work reported here, we expect this might be close to 15 650 $cm^{-1}$ before accounting for solvent shifts. Second, a closer investigation of the weak undulations present on the red wing of the Chappuis system seems warranted. The spectrum appears to be characterized by complex isotope shifts, some of which are related to the Wulf band system. Such behavior might point to the participation of yet another electronic state in this region. Third, the isotope shifts of the Hartley band oscillations should be measured. One might expect the shifts for the long-period orbits, which explore the wells on the $^1B_2$ surface, to be relatively large compared with those associated with the shortest period orbit since the latter correspond to nearly pure $\nu_1$ motion along the axis of the $C_{2v}$ saddle. These data would provide an interesting test of the recent assignment based on the autocorrelation method. Last, but perhaps most important, it is hoped that this work will help motivate new *ab initio* calculations for the potential energy surfaces associated with the visible absorption bands of ozone.

## ACKNOWLEDGMENTS

This work was supported by a grant from NASA's upper atmosphere research program. We thank Mr. J. Morton for technical assistance, and Dr. R. T Pack for examining the impact of isotopic labeling on his spectroscopic model and numerous stimulating conversations.

[1] M. J. Chappuis, C. R. Acad. Sci. (Paris) **91**, 985 (1880).
[2] O. R. Wulf, Proc. Nat. Acad. Sci. **16**, 507 (1930).
[3] E. C. Y. Inn and Y. Tanaka, J. Opt. Soc. Am. **43**, 870 (1953).
[4] M. Griggs, J. Chem. Phys. **49**, 857 (1968).
[5] E. Vigroux, Ann. Phys. (Paris) **8**, 709 (1953).
[6] G. L. Humphrey and R. M. Badger, J. Chem. Phys. **15**, 794 (1947).

[7] O. R. Wulf, Ann. Astrophys. Observatory of the Smithsonian Institution, **7**, 177 (1954).
[8] P. Rigaud, J. P. Naudet, and D. Huguenin, J. Geophys. Res. **88**, 1463 (1983).
[9] H. B. Levene, J.-C. Nieh, and J. J. Valentini, J. Chem. Phys. **87**, 2583 (1987).
[10] J. I. Steinfeld, S. M. Adler-Golden, and J. W. Gallagher, J. Phys. Chem. Ref. Data **16**, 911 (1987).
[11] P. J. Hay and W. A. Goddard III, Chem. Phys. Lett. **14**, 46 (1972).
[12] P. J. Hay and T. H. Dunning, Jr., J. Chem. Phys. **67**, 2290 (1977).
[13] V. Vaida, D. J. Donaldson, S. J. Strickler, S. L. Stephens, and J. W. Birks, J. Phys. Chem. **93**, 506 (1989).
[14] D. H. Katayama, J. Chem. Phys. **71**, 815 (1979); **85**, 6809 (1986).
[15] S. M. Anderson, J. Morton, and K. Mauersberger, J. Chem. Phys. **93**, 3826 (1990).
[16] J. Reader and C. H. Corliss, *Wavelengths and Transition Probabilities for Atoms and Atomic Ions I. Wavelengths* (U.S. Nat. Bur. Stds., U.S. Dept. of Commerce, Washington, D.C.), pp. 10–11, 86–87.
[17] G. D. Greenblatt, J. J. Orlando, J. B. Burkholder, and A. R. Ravishankara, J. Geophys. Res. **95**, 18,577 (1990).
[18] G. Herzberg, *Molecular Spectra and Molecular Structure, III. Electronic Spectra and Electronic Structure of Polyatomic Molecules* (Van Nostrand Reinhold, New York, 1966); p. 142 ff.
[19] There appears to be a systematic wavelength error in Ref. 13. The wavelengths of bands $1a$ and $X$ in the gas-phase spectra are given there as 597 and 568 nm, whereas the literature values (and ours) are consistently 5 nm larger. The frequencies as given here from Ref. 13 assume a simple 5 nm correction applies to all of their values.
[20] G. W. Robinson, J. Chem. Phys. **46**, 572 (1967).
[21] K.-H. Thunemann, S. G. Peyerimhoff, and R. J. Buenker, J. Mol. Spectrosc. **70**, 432 (1978).
[22] P. J. Hay (personal communication).
[23] R. T Pack, J. Chem. Phys. **65**, 4765 (1976).
[24] R. T Pack (personal communication).
[25] E. J. Heller, Acc. Chem. Res. **14**, 368 (1981).
[26] B. R. Johnson and J. L. Kinsey, Phys. Rev. Lett. **62**, 1607 (1989).